



# ZSCAN1 Autoantibodies Are Associated with Pediatric Paraneoplastic ROHHAD

Caleigh Mandel-Brehm, PhD <sup>1†</sup> Leslie A. Benson, MD,<sup>2†</sup> Baouyen Tran, PhD <sup>3†</sup>  
 Andrew F. Kung, BA,<sup>1</sup> Sabrina A. Mann, BS,<sup>1</sup> Sara E. Vazquez, BS,<sup>1</sup> Hanna Retallack, PhD,<sup>1</sup>  
 Hannah A. Sample, BS <sup>1</sup> Kelsey C. Zorn, MHS,<sup>1</sup> Lillian M. Khan, BS,<sup>1</sup> Lauren M. Kerr, BA,<sup>4</sup>  
 Patrick L. McAlpine, BS,<sup>5</sup> Lichao Zhang, PhD,<sup>6</sup> Frank McCarthy, BS,<sup>6</sup> Joshua E. Elias, PhD,<sup>6</sup>  
 Umakanth Katwa, MD,<sup>7</sup> Christina M. Astley, MD, ScD <sup>8</sup> Stuart Tomko, MD,<sup>9</sup>  
 Josep Dalmau, MD, PhD,<sup>10</sup> William W. Seeley, MD,<sup>11</sup> Samuel J. Pleasure, MD, PhD,<sup>3</sup>  
 Michael R. Wilson, MD,<sup>12</sup> Mark P. Gorman, MD,<sup>2‡</sup> and Joseph L. DeRisi, PhD<sup>13‡</sup>

**Objective:** Rapid-onset Obesity with Hypothalamic Dysfunction, Hypoventilation and Autonomic Dysregulation (ROHHAD), is a severe pediatric disorder of uncertain etiology resulting in hypothalamic dysfunction and frequent sudden death. Frequent co-occurrence of neuroblastic tumors have fueled suspicion of an autoimmune paraneoplastic neurological syndrome (PNS); however, specific anti-neural autoantibodies, a hallmark of PNS, have not been identified. Our objective is to determine if an autoimmune paraneoplastic etiology underlies ROHHAD.

**Methods:** Immunoglobulin G (IgG) from pediatric ROHHAD patients (n = 9), non-inflammatory individuals (n = 100) and relevant pediatric controls (n = 25) was screened using a programmable phage display of the human peptidome (PhIP-Seq). Putative ROHHAD-specific autoantibodies were orthogonally validated using radioactive ligand binding and cell-based assays. Expression of autoantibody targets in ROHHAD tumor and healthy brain tissue was assessed with immunohistochemistry and mass spectrometry, respectively.

**Results:** Autoantibodies to ZSCAN1 were detected in ROHHAD patients by PhIP-Seq and orthogonally validated in 7/9 ROHHAD patients and 0/125 controls using radioactive ligand binding and cell-based assays. Expression of ZSCAN1 in ROHHAD tumor and healthy human brain tissue was confirmed.

**Interpretation:** Our results support the notion that tumor-associated ROHHAD syndrome is a pediatric PNS, potentially initiated by an immune response to peripheral neuroblastic tumor. ZSCAN1 autoantibodies may aid in earlier, accurate diagnosis of ROHHAD syndrome, thus providing a means toward early detection and treatment. This work warrants follow-up studies to test sensitivity and specificity of a novel diagnostic test. Last, given the absence of the ZSCAN1 gene in rodents, our study highlights the value of human-based approaches for detecting novel PNS subtypes.

ANN NEUROL 2022;92:279–291

View this article online at [wileyonlinelibrary.com](https://www.wileyonlinelibrary.com). DOI: 10.1002/ana.26380

Received Nov 22, 2021, and in revised form Apr 18, 2022. Accepted for publication Apr 21, 2022.

Address correspondence to DeRisi, 1700 4th street, QB3 room 404, San Francisco, CA 94110. E-mail: [joe@derisilab.ucsf.edu](mailto:joe@derisilab.ucsf.edu) and Gorman, 300 Longwood Ave, Boston, MA. E-mail: [mark.gorman@childrens.harvard.edu](mailto:mark.gorman@childrens.harvard.edu)

<sup>†</sup>Authors contributed equally to this work.

<sup>‡</sup>Authors contributed equally to this work; Co-Corresponding authors.

From the <sup>1</sup>Department of Biochemistry and Biophysics, University of California, San Francisco, CA, USA; <sup>2</sup>Department of Neurology, Harvard Medical School, Boston, MA, USA; <sup>3</sup>Weill Institute for Neurosciences, Department of Neurology, University of California, San Francisco, CA, USA; <sup>4</sup>Department of Neurology, Boston Children's Hospital, Boston, MA, USA; <sup>5</sup>Otolaryngology Head and Neck Surgery Research Division, Stanford University, Stanford, CA, USA; <sup>6</sup>Chan Zuckerberg Biohub, Stanford, CA, USA; <sup>7</sup>Department of Pulmonary Medicine, Sleep Center, Boston Children's Hospital, Boston, MA, USA; <sup>8</sup>Division of Endocrinology & Computational Epidemiology, Boston Children's Hospital, Boston, MA, USA; <sup>9</sup>Department of Neurology, Washington University, St. Louis, MO, USA; <sup>10</sup>Catalan Institution for Research and Advanced Studies (ICREA), Hospital Clinic-Idibaps, University of Barcelona, Barcelona, Spain; <sup>11</sup>Memory and Aging Center, Department of Neurology, University of California, San Francisco, CA, USA; <sup>12</sup>MAS, Weill Institute for Neurosciences, Department of Neurology, University of California, San Francisco, CA, USA; and <sup>13</sup>Chan Zuckerberg Biohub, Department of Biochemistry and Biophysics, University of California, San Francisco, CA, USA

Additional supporting information can be found in the online version of this article.

**R**apid-onset Obesity with Hypothalamic Dysfunction, Hypoventilation and Autonomic Dysregulation (ROHHAD) is a poorly understood pediatric syndrome with high morbidity and mortality, distinguished by its unique progression of multi-system derangements.<sup>1, 2</sup> Variable degrees of hypothalamic and presumed brainstem dysfunction manifest after age 2 as obesity, autonomic dysregulation, and alveolar hypoventilation with risk of sudden death from respiratory or autonomic dysfunction.<sup>1–6</sup> Neuropsychiatric changes and seizures have been described.<sup>7, 8</sup> Detailed longitudinal follow up describing ROHHAD's natural history is limited.<sup>9</sup> Although incurable, early supportive care including respiratory support for hypoventilation may reduce morbidity.<sup>10, 11</sup> Diagnosis remains difficult given lack of biomarkers and overlap with other pediatric disorders, including congenital central hypoventilation syndrome (CCHS), Prader-Willi syndrome, and other forms of genetic and non-genetic obesity.<sup>12–15</sup> Although recognized as a distinct disorder since 2000, ROHHAD is rare with fewer than 200 reported cases.<sup>1, 5</sup> The etiology is unclear.

Thus far, most etiologic investigations into ROHHAD have focused on genetic susceptibility, without consistent results.<sup>16–19</sup> The presence of neuroblastic tumor (NT, including neuroblastoma, ganglioneuroblastoma, ganglioneuroma) defines a large subset of patients with ROHHAD (30–100%, depending on the series), sometimes referred to as ROHHAD-NET.<sup>5, 20</sup> NTs are similarly associated with CCHS, a genetic condition due to mutations in PHOX2B, and opsoclonus-myoclonus syndrome (OMS), an autoimmune paraneoplastic neurological syndrome (PNS).<sup>21–23</sup> With respect to ROHHAD, several observations suggest an immune-mediated disease, including the presence of oligoclonal bands in cerebrospinal fluid (CSF) and immune-cell infiltrates in brain, including hypothalamus and brainstem at autopsy.<sup>24–29</sup> In addition, some patients with ROHHAD have variable improvement with immunosuppressive therapy.<sup>30, 31</sup> Establishing ROHHAD as a PNS would have important implications for developing diagnostic biomarkers, highlighting the need for tumor identification and resection, and advancing the use of immunosuppressive treatments.<sup>32</sup>

On a molecular level, a PNS can be defined by its association with autoantibodies to specific onconeural antigens, or proteins expressed in both the pathogenic tumor and healthy nervous system.<sup>33</sup> Despite a suspicion of PNS in ROHHAD, evidence of anti-neural reactivity is limited and an associated onconeural antigen has not been identified.<sup>29, 34</sup> Here, we deployed human-specific phage-display immunoprecipitation and next-generation sequencing (PhIP-Seq) and complementary techniques to investigate a possible paraneoplastic etiology in ROHHAD. We find

that immunoglobulin (Ig) G autoantibodies to protein Zinc finger and SCAN domain-containing protein 1 (ZSCAN1) are robustly associated with ROHHAD and may be useful as a diagnostic biomarker and advancing knowledge of this poorly understood disease.

## Methods

All relevant ethical regulations were followed regarding animal experiments and human research participant involvement. For animal experiments, protocols were approved by the Institutional Animal Care and Use Committee. For human samples, we have obtained informed consent from all participants and/or their parents.

### Patient Recruitment

All local Institutional Review Board (IRB) regulations were followed at Boston Children's Hospital (BCH) (protocol #09-02-0043) and University of California, San Francisco (protocol #13-12236). All patient specific data were extracted by chart review (L.B., L.K., S.T.) and samples obtained following family consent. ROHHAD subjects were identified by pediatric neuro-immunologists (L.B. or S.T.) on the basis of clinical suspicion for ROHHAD syndrome, without alternative diagnosis. Eight of nine patients (ROHHAD-7 excluded) met criteria used to definite ROHHAD syndrome.<sup>2</sup> Three patients were initially screened in a pilot study, 5 more Boston Children's and 1 Washington University patients' samples were subsequently obtained and added. Between 2010 and 2022 at BCH, one author (L.B.) evaluated 21 patients for possible ROHHAD syndrome, of whom 9 had a definite diagnosis, 8 of which were known to have tumors. Of these 9 patients, 8 had available samples for inclusion in the current study.

### Autoantibody Discovery and Validation

For autoantibody discovery, we used the PhIP-Seq library and experimental protocol as previously described.<sup>35</sup> PhIP-seq datasets were analyzed with a formalized analysis pipeline (generated in-house) that includes alignment of DNA reads to input library, conversion to peptide reads, summing of peptides by protein ID, normalization to 100,000 reads (RP100K), and calculating mean RP100K for each protein. Alignment of sequencing reads to the input library on a peptide-level was performed with RAP-search2<sup>36</sup> and command line “/data/bin/rapsearch -d input\_library -q read1\_location -o output\_location -z 12 -v 1 -b 0.” A Z-score enrichment for each protein was calculated based on mean RP100K generated from a large set of healthy controls. Z-score formula = (proteinX mean RP100K<sub>Experimental</sub> – proteinX mean RP100K<sub>control</sub>) / (Standard Deviation of proteinX in controls).

### **293T Cell-Based Assay: Immunocytochemistry and Imaging**

The 293T cell-based assay (CBA) transfections, immunocytochemistry, and imaging were performed as previously described.<sup>35</sup> Cells were stained according to standard procedure with one of the following primary antibodies: Patient IgG (CSF 1:100, Serum 1:1000), commercial anti-ZSCAN1 IgG (1 µg/mL), or commercial anti-FLAG IgG (1 µg/mL), followed by staining with an appropriate secondary antibody (anti-human IgG Alexa 488, anti-rabbit IgG, or anti-mouse IgG Alexa 568). Images were captured using a Nikon Ti CSU-W1 Spinning Disk/High Speed Widefield microscope at the UCSF Nikon Core Facility with a Plan Apo 20x/0.75 or Plan Apo VC 100x/1.4 oil immersion lens. Image capture settings, including exposure time, laser intensity, aperture, and magnification, were kept constant for all conditions in the experiment and analyzed in ImageJ.

### **293T CBA: Slot-Blot Western Blotting**

Twenty-four hours post-transfection, cells were washed once in cold 1× phosphate buffered saline (PBS), then harvested and lysed with RIPA buffer for 30 minutes at 4°C with gentle agitation. Lysates were spun down for 30 minutes at 16,000 × g at 4°C. Supernatants were diluted to a 1 mg/mL protein concentration using the BCA (Pierce) kit and prepared for sodium dodecyl sulfate/polyacrylamide gel electrophoresis (SDS/PAGE) and slot-blot Western blotting. The 4× Laemmli buffer was added to lysates, boiled for 5 minutes at 95°C, loaded onto a 4–12% gradient SDS-PAGE gel (Bio-Rad), then transferred to a 0.20 micron polyvinylidene difluoride (PVDF) membrane. Membranes were blocked at room temperature for 2 hours in blocking buffer (LI-COR), then loaded onto a multiscreen apparatus to screen for multiple CSF or serum samples as well as commercial antibodies. Human CSF samples were loaded at 1:200, human serum samples were loaded at 1:10000, while commercial antibodies were loaded at 1:2000 and incubated overnight at 4°C. To visualize proteins of interest, anti-human IgG (LI-COR 680) and anti-rabbit IgG (LI-COR 800) were loaded into wells and incubated for 2 hours at room temperature and scanned on Odyssey imaging system (LI-COR).

### **Onconeural Antigen Investigation**

To examine candidate autoantigen expression in ROHHAD tumor and healthy human brain, we used immunohistochemistry and immunoprecipitation-mass spectrometry (IP-MS), respectively. For tumor examination, fresh frozen tumor was embedded, sectioned, fixed on slides, stained, and imaged according to standard procedures. To detect ZSCAN1, we immunostained with

commercial antibody to ZSCAN1 (rabbit, Thermo Fisher Scientific, PA552488) and anti-rabbit secondary. For IP-MS experiments, ~100 mg of frozen human hypothalamus was homogenized and prepared for IP and subsequent MS analysis. For IP, lysate was diluted to 0.5 mg/mL and 1 of the following antibodies was added at 1 µg/mL: rabbit anti-ZSCAN1 (Thermo Fisher Scientific, PA552488), rabbit anti-ZSCAN1 (Sigma Aldrich HPA007938), rabbit IgG control (Thermo Fisher Scientific, 31235). Positive identification of ZSCAN1 required detection with 2 commercial antibodies and absence from isotype control. Two technical replicates were performed.

### **Mass Spectrometry Analysis**

The protein bound magnetic beads were resuspended in 100 µL of 0.1% RapiGest SF Surfactant (Waters, Milford, MA) in 100 mM ammonia bicarbonate. The proteins were reduced (5 mM dithiothreitol, 37°C, 60 min) and alkylated (14 mM iodoacetamide, room temperature in dark, 45 min). Five microgram of trypsin was added to each sample for digestion overnight at 37°C. Peptide-containing supernatant was separated from the magnetic beads, and trifluoroacetic acid was added to the supernatant to adjust the pH to below 2. The sample was incubated at 37°C for 30 minutes followed by centrifugation at 16,000 rcf for 10 minutes, and subject to desalting with RP-S cartridges on an AssayMAP Bravo platform (Agilent, Santa Clara, California) and resuspended in 0.1% formic acid.

Desalted peptides were analyzed on a Fusion Lumos mass spectrometer (Thermo Fisher Scientific, San Jose, CA) equipped with a Thermo EASY-nLC 1200 LC system (Thermo Fisher Scientific, San Jose, CA). Peptides were separated by capillary reverse phase chromatography on a 25 cm column (75 µm inner diameter, packed with 1.6 µm C18 resin, AUR2-25075C18A, Ionopticks, Victoria Australia). Peptides were introduced into the Fusion Lumos mass spectrometer using a gradient with 3–27% buffer B (0.1% (v/v) formic acid in acetonitrile) for 105 minutes followed by 27–40% buffer B for 15 minutes at a flow rate of 300 nL/min. Data were acquired in top speed data dependent mode with a duty cycle time of 1 second. Selected precursor ions from MS1 were subjected to fragmentation using higher-energy collisional dissociation (HCD) with quadrupole isolation window of 0.7 m/z, and normalized collision energy of 31%. HCD fragments were analyzed in the Ion Trap. Fragmented ions were dynamically excluded for a period of 45 seconds.

The resulting data were searched using SEQUEST HT on the Proteome Discoverer (2.2.0.388) platform, against a database combining Human proteins (downloaded

January 28, 2021) and common contaminants. The precursor mass range was set to 350–5,000 Da, the mass error tolerance was set to 10 ppm, and the fragment mass error tolerance to 0.6 Da. Enzyme specificity was set to trypsin, carbamidomethylation of cysteines (+57.021) was set as fixed modifications, oxidation of methionines (15.995) and acetylation of protein N-terminus (+42.011) was considered as variable modifications. Percolator was used to filter peptides and proteins to a false discovery rate of 1%. Abundance quantification was based on precursor ion intensities.

### **Animal Protocol**

All animal protocols were in accordance with the regulations of the National Institute of Health and approved by the University of California San Francisco Institutional Animal Care and Use Committee (IACUC). Wild-type C57BL/6J mice were obtained from Jackson Laboratories (Bar Harbor, ME, USA). Adult mice (> postnatal day 42) were used for immunohistological screening of human patient antibodies.

### **Radioligand Binding Assay**

The radioligand binding assay (RLBA) was performed as described previously.<sup>43</sup> Briefly, full-length human ZSCAN1 was in vitro transcribed and translated with [<sup>35</sup>S]-methionine in a T7 dependent system using a ZSCAN1 plasmid containing a T7 promoter (Origene Cat: RC221074). The radiolabeled ZSCAN1 protein was then column purified and immunoprecipitated with 2.5 μL of serum or CSF per well using Sephadex protein A/G beads (Sigma Aldrich, St. Louis, MO; #GE17-5280-02 and #GE17-0618-05) in 96-well filtration plates (Corning, Corning, NY; #EK-680860). The plates were read out as counts per minute (cpm) using the Microbeta Trilux liquid scintillation plate reader (Perkin Elmer).

### **Data Availability**

Original data contributing to the main findings in our study as well as additional supplementary figures and tables are provided on Dryad repository (temporary link for review: <https://datadryad.org/stash/share/P0zU0SM4Oth44F35oirk6pJhBFjCgghDSByaCc2jWM>). The dryad repository includes raw data for PhIP-Seq analysis, RLBA analysis, mass spectrometry, immunohistochemistry images, and Western blots. There are no data restrictions for this study.

## **Results**

### **Clinical Profile of ROHHAD Cohort**

The ROHHAD cohort consisted of nine patients (ROHHAD-1 through -9) selected on the basis of clinical suspicion for ROHHAD syndrome, without alternative diagnosis (Table). Each patient was found to exhibit

defining features of ROHHAD syndrome including rapid-onset of obesity between 2 and 5 years of age and multiple additional features of hypothalamic dysfunction. Three patients were described previously.<sup>1, 7, 37</sup> Hypoventilation was present in 8/9 at diagnosis. Eight of nine patients were found to have NT (ROHHAD-1 through 8), while a single patient in this cohort was not known to have a tumor (ROHHAD-9), although work-up was limited to chest x-ray and chest MRI without abdominal imaging. Eight of nine subjects had clinical genetic testing without genetic syndromes identified to explain their phenotypes, including 8/9 with dedicated or whole exome testing ruling out PHOX2B mutations. Features suggestive of a neuroinflammatory process include comorbid autoimmune diseases (2/9), elevated CSF neopterin (3/9), and CSF-specific oligoclonal bands (1/8 tested). Improvement in symptoms was observed in 6/7 patients treated acutely with supportive care, tumor resection and immunosuppressive therapy at diagnosis. Response to immunosuppressive therapy was most clearly demonstrated in ROHHAD-6 in whom CO<sub>2</sub> retention improved and worsened in parallel with changing steroid doses. Similarly, neurobehavioral symptoms improved for ROHHAD-7.<sup>7</sup> Additional clinical details pertaining to autoimmune features and neurologic phenotypes for the ROHHAD cohort are provided in supplemental Tables S1 and S2, respectively.

### **Clinical Profile of Control Cohorts**

Control cohort 1 (CC1) and control cohort 2 (CC2) were assembled for PhIP-Seq screening and validation experiments, respectively. Clinical details and demographics pertaining to controls is provided in supplemental Table S3 (CC1) and supplemental Table S4 (Pediatric controls OMS and Obesity +NT).

### **Screening for Autoantibodies Using Rodent-Based Approaches**

Immunohistochemical screening of patient antibodies against neural tissue, typically rodent, is a classical approach for identifying cryptic autoimmune etiologies among idiopathic neurological syndromes.<sup>38–41</sup> In two independent laboratories (J.D.R., S.J.P.), antibodies in CSF from ROHHAD-1 through -6 were tested for immunoreactivity against mouse brain tissue. Neither identified anti-neural reactivity in any patient. Additional, independent assessment of autoantibodies to extracellular neural targets were also tested in 4 patients in this cohort using pre-established protocols for fixed and live rat neurons<sup>41, 42</sup> (see supplemental Table S1). All studies were negative (negative data pertaining to immunohistochemistry using rodent based approaches available on Dryad).

**TABLE. Clinical profile of ROHHAD cohort.**

Patient No. (Age at Onset & Sex)	Age (yrs) ROHHAD suspected	Age (yrs) at Sample Collection	Age at Onset Obesity (z-score)	Respiratory phenotype	Endocrinop- athies	Autonomic Dysfunction	Tumor Type (age at identification)	CSF Results	Outcome
1 (2yrF)	9	10.1 (CSF), 10.6 (Serum)	2 yr (Z = +2.7 at 9y)	CSA, 24 hour HV	Yes	Yes	Ganglio-neuroma (9 yr)	1 WBC/m <sup>3</sup> , 8 RBC/m <sup>3</sup> , 0 OCBs	Alive, 17yr
2 (5yrF) <sup>37</sup>	6	6.0 (CSF), 6.0 (serum)	5 yr (Z = +2.9 at 6 yr)	Night-time HV	Yes	Yes	Ganglio-neuroma (6 yr)	0 WBC/m <sup>3</sup> , 54 RBC/m <sup>3</sup> , 0 unique CSF OCB	Alive, 13yr
3 (2yrM)	3	3.2 (Serum) 4.0 (CSF)	2 yr (Z = +5, 2at 2y)	CSA, 24 hour HV	Yes	Yes	Neuro-blastoma (3 yr)	5 WBC/m <sup>3</sup> , 525 RBC/m <sup>3</sup> , 13 OCBs at diagnosis; 4 OCB after 10 months; 2 OCB and neopterin of 75 (el) after 2.5 years)	Sudden death 8yr
4 (2yrM)	2	2.7 (Serum) 2.7 (CSF), 2.6 (Tumor)	2 yr (Z = +2.1 at 2y)	CSA, 24 hour HV	Yes	Yes	Ganglio-neuro- blastoma (2 yr)	4 WBC/m <sup>3</sup> , 2 RBC/m <sup>3</sup> , 2 OCBs (nl), neopterin 20 (nl)	Alive 4yr
5 (3yrM)	3	3.8 (Serum) 3.8 (CSF), 3.8 (Tumor)	3 yr Z = +5.2 at 3y)	CSA, 24 hour HV	Yes	Yes	Ganglio-neuro- blastoma (3yr)	0 WBC/m <sup>3</sup> , 0 RBC/m <sup>3</sup> , 0 OCBs, Neopterin 41 (nl) (repeat after 5.5 months similar)	Alive 5yr, severely debilitate-ed, immobile, severe behavior problems
6 (3yrM)	5	5.2 (CSF), 5.2 (Serum)	3 yr(Z = +3.9 at 5y)	24 hour HV	Yes	Yes	Ganglio-neuro-blastoma, intermixed (5yr)	36 WBC/m <sup>3</sup> , 0 RBC/m <sup>3</sup> , 0 OCBs, Neopterin 94 (el)	Alive 6yr
7 (2yrF) <sup>7</sup>	4	11 (Serum)	2 yr	OSA	Yes	No	Ganglio-neuro- blastoma (3 yr)	Not tested	Alive 11yr
8 (3yrF) <sup>1</sup>	8	24.1 (Serum) 25.2 (CSF)	3 yr	24 hour HV	Yes	No	Ganglio- neuroma (7 yr)	2 WBC/m <sup>3</sup> , 60 RBC/m <sup>3</sup> , 141 protein, 0 OCBs, Neopterin 21 (nl)	Alive 30yr
9 (3yrM)	12	7.5 (Serum)	3 yr (Z = +4.7 at 4y)	CSA, 24 hour HV	Yes	No	None (abdomen not imaged)	2 WBC/m <sup>3</sup> , 31 RBC/m <sup>3</sup> , 0 unique CSF OCB, Neopterin 76 (el)	Sudden death 13yr

CSF = Cerebrospinal Fluid, CSA = central sleep apnea, el = elevated, HV = hypoventilation, nl = normal, OCB = Oligoclonal Band, OSA = Obstructive Sleep Apnea, Yr = years. \*All tested CSF had normal protein, glucose and IgG index values except where noted. #Endocrine and other symptomatic treatment not recorded. Further details on ROHHAD phenotypes in supplemental tables.

### Screening for Autoantibodies Using Human-Specific PhIP-Seq

The PhIP-Seq library employed here displays a representation of the human proteome and has been used previously for detecting diagnostic PNS autoantibodies.<sup>35, 43</sup> As part

of a discovery pilot, we screened CSF from 3 ROHHAD patients (ROHHAD-1 through 3) and plasma from CC1 (n = 100). CC1 represents plasma from 100 de-identified blood donors courtesy of New York Blood Center. Individual PhIP-Seq experiments were sequenced with the

total number of DNA reads normalized to 100,000 reads, referred to as RP100K, to enable comparison of protein enrichments. An RP100K for each protein in the library was generated for each patient, then averaged according to cohort. To aid in candidate identification, ROHHAD-specific Z-score enrichments for each protein were generated, using CC1 values (see the Methods section). All proteins with a ROHHAD mean RP100K > 0 were plotted relative to Z-score enrichments (Fig 1). Candidate antigens were expected to satisfy the following criteria in at least 2 patients: a minimum level of recovery (RP100K > 50) and minimum Z-score enrichment (>3). Of the ~20,000 protein possibilities, only 1 protein, ZSCAN1, satisfied these criteria. Using the same criteria above, enrichment of ZSCAN1 was not observed in other previously published autoimmune cohorts screened on the same PhIP-Seq platform, including PNS syndromes anti-Yo (n = 36), anti-Hu (n = 44), anti-Ma2 (n = 2), anti-KLHL11 (n = 7), or patients with systemic Autoimmune Polyglandular Syndrome Type I (n = 39).<sup>35, 43, 44</sup>

### Orthogonal Validation Assays

To further investigate the association of ZSCAN1 and ROHHAD syndrome, we repeated PhIP-seq with an expanded ROHHAD cohort (including the 3 original patients) and new set of controls (CC2). CC2 represents 27 de-identified healthy volunteers (plasma n = 3; sera n = 17, CSF n = 7) and 26 clinically relevant pediatric controls. Pediatric controls include childhood obesity +

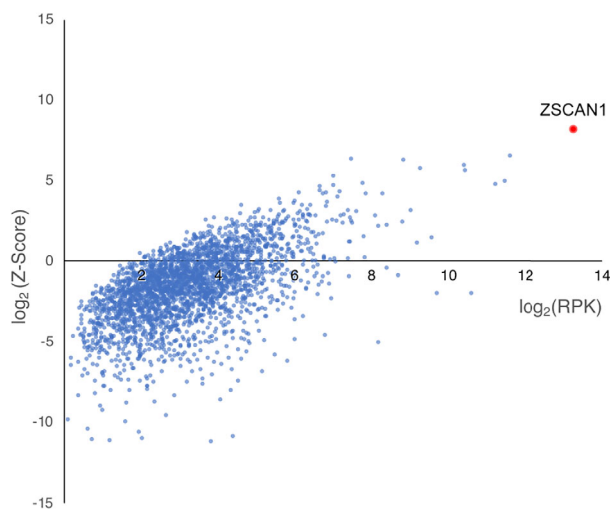


**FIGURE 1:** PhIP-Seq screen implicates ZSCAN1 as a candidate autoantigen in ROHHAD. CSF from 3 ROHHAD patients (ROHHAD-1 to -3) and plasma from a large set of “healthy controls” (n = 100) were tested by PhIP-Seq. Individual data were averaged according to cohort. All proteins with a ROHHAD mean RP100K > 0 are plotted against ROHHAD Z-score enrichments compared to healthy controls. Non-ZSCAN1 proteins are denoted with blue dots; ZSCAN1 is denoted with a red dot.

NT (n = 1), and children with OMS (with NT n = 10, without NT n = 15). For all samples, ZSCAN1 RP100K is reported, as well as, Z-score enrichment based on our background control dataset CC1 (ZSCAN1 mean = 8.18 RP100K, standard deviation = 32.53 RP100K), with Z-score >3 considered positive. We reproduced the association between ZSCAN1 and ROHHAD, showing enrichment in 7 of 9 ROHHAD patients (ROHHAD-1 to -7) and 0 of 50 samples from CC2 (Fig 2A). We next leveraged peptide-level data and found antigenicity within ZSCAN1 was largely restricted to the C-terminal of ZSCAN1, with patients displaying enrichment of overlapping peptides, increasing confidence in our findings (Fig 3). Intriguingly, patients ROHHAD-1 through -7 shared an antibody that bound to a common 11 amino acid (AA) epitope.

To confirm ZSCAN1 enrichment in our ROHHAD cohort, we tested for IP of recombinant ZSCAN1 in two orthogonal assays, including a radioligand binding assay (RLBA) and 293 T cell-based overexpression assay (CBA). For the six patients with paired CSF and sera (ROHHAD 1 through 6), ZSCAN1 enrichment in one sample type was sufficient to be called positive in a given assay. First, the RLBA with in vitro transcribed and translated full-length ZSCAN1 protein revealed positive IP (fold-change >10) by ROHHAD patients 1 through 7 (sera n = 7/7; paired CSF n = 6/6) and no enrichment in CC2 healthy controls (Fig 2B). Low-level enrichment of ZSCAN1 was observed in two patients negative by PhIP-Seq; ROHHAD-9 and OMS-4. Second, using immunocytochemistry and 293T cells expressing full-length ZSCAN1, we show colocalization of human antibodies with commercial antibody to ZSCAN1 for ROHHAD patients 1 through 7 (sera n = 2 ROHHAD-1 and 3; CSF n = 6 ROHHAD-1 through -6). Co-localization is not observed for ROHHAD-8, ROHHAD-9, or controls, including OMS-4 (Fig 2C). Taken together, ROHHAD-1 through -7 reproduced ZSCAN1 enrichment in 2 antibody-based orthogonal assays, thus limiting possibility of false-positives and validating autoantibodies to ZSCAN1 in this cohort.<sup>45</sup>

Of note for 293T CBAs, we observed increased sensitivity to ZSCAN1 autoantibody detection using CSF compared to sera. This is exemplified best in data collected from the 6 patients with paired CSF and sera (ROHHAD-1 through -6). In 293T CBAs, ZSCAN1 autoantibodies were detected using 6/6 CSF samples (Fig 4A). In contrast, only 2/6 paired sera were positive (Fig 4B). To rule out technical artifacts, sera samples were re-tested on CBA at several dilutions 1:100, 1:1000, 1:2000, and 1:5000, with no change in seronegativity. We further tested for recognition of ZSCAN1

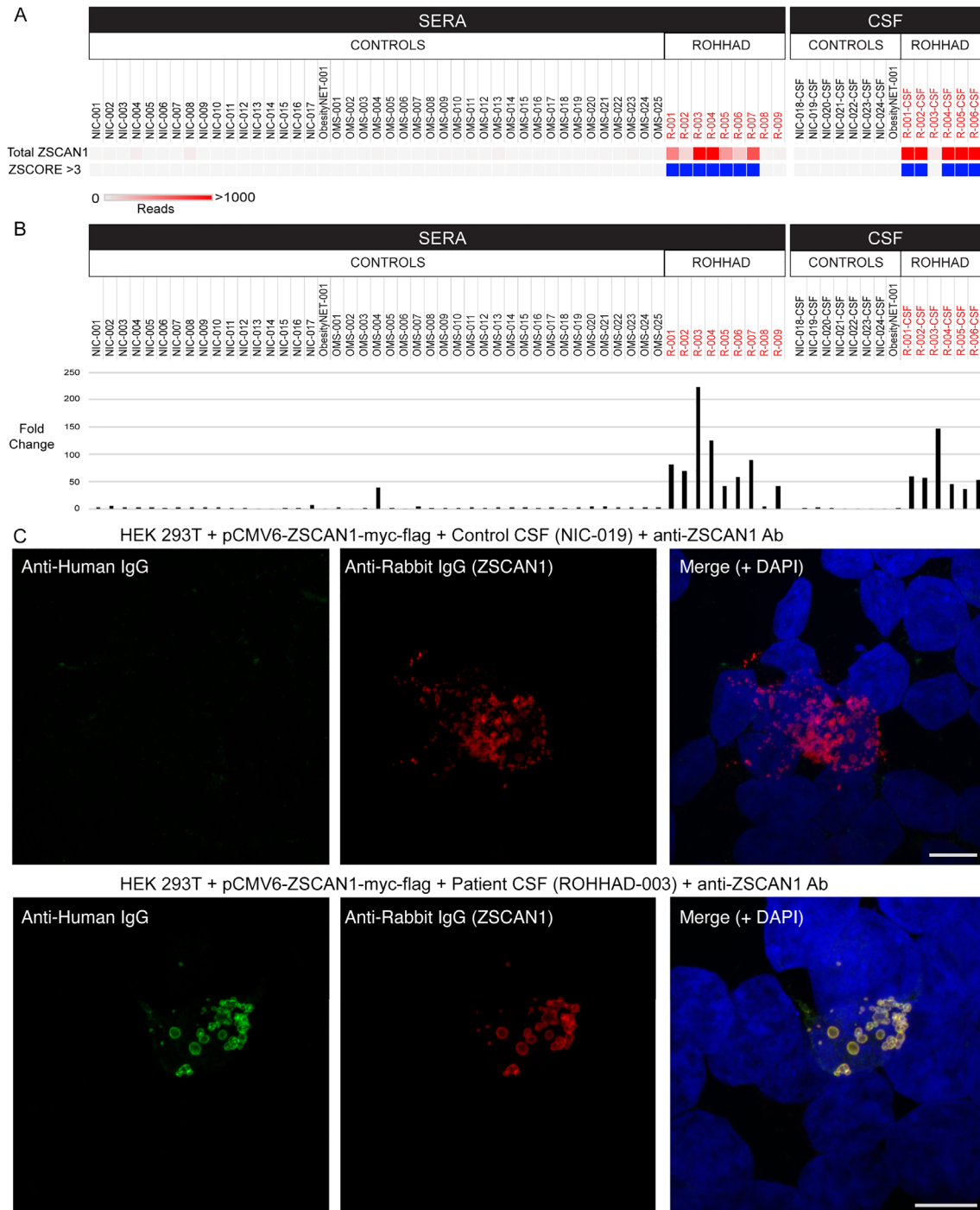


**FIGURE 2: Validation of autoantibodies to ZSCAN1 in ROHHAD patients.** In panel a and b, enrichment of ZSCAN1 by PhIP-Seq and RLBA was compared between ROHHAD patients ( $n = 9$ ), non-inflammatory healthy controls ( $n = 24$ ), and pediatric controls including children with OMS with and without NT ( $n = 25$ ) and an obesity patient with NT ( $n = 1$ ). Data represent the average of 2 independent technical replicates. a, PhIP-Seq analysis. Each column represents an individual sample. A heatmap of total ZSCAN1 RP100K is shown in the top row. To enable comparisons between the majority of samples with lower signal we added a ceiling value of 1,000 RP100K. Z-Score enrichments based on our 100 human donor dataset are plotted below, with samples that have Z-score enrichments  $>3$  colored with blue squares. Gray squares indicate Z-score  $<3$ . b, RLBA testing immunoprecipitation of recombinant ZSCAN1 by ROHHAD patients and controls. For all samples, fold change was calculated by dividing by the mean value from control sera ( $n = 17$ , mean = 20.83). c, Representative image showing immunostaining of 293T cells expressing full-length ZSCAN1 with human CSF and commercial antibody to ZSCAN1 (rabbit). Top row shows immunostaining with control CSF. Bottom row shows staining with ROHHAD-3 CSF. Colocalization is indicated by yellow in the merge images (far right both rows).

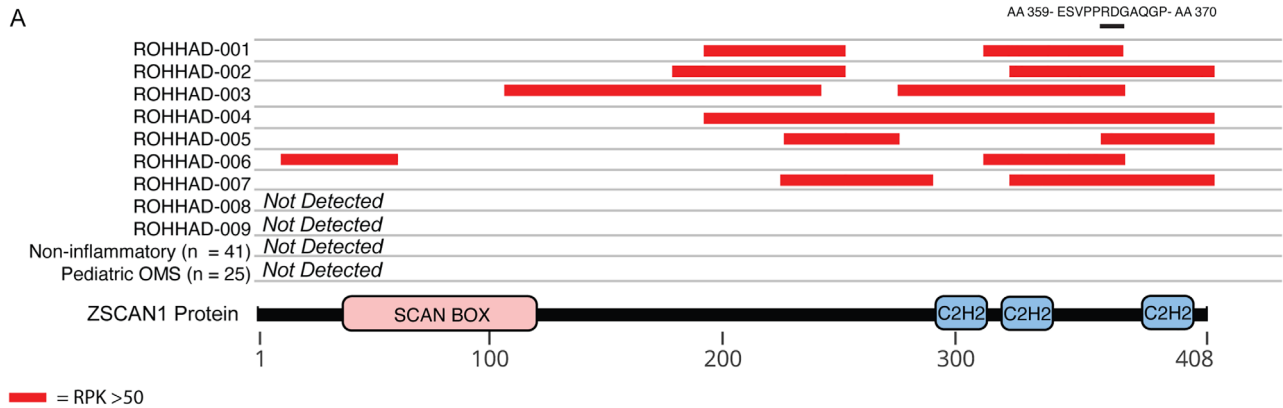


**FIGURE 3: Peptide-level ZSCAN1 enrichments by ROHHAD patients, informed by PhIP-Seq.** Cartoon graphic of the 408 amino acid ZSCAN1 protein with annotated SCAN and C<sub>2</sub>H<sub>2</sub> domains is depicted below. Horizontal tracks above ZSCAN1 represent peptide enrichment data from individual ROHHAD patients or aggregated data from control cohorts. All peptides belonging to ZSCAN1 with enrichment RP100K >50 were plotted as red bars, merging together peptides with overlapping regions within individual tracks to reflect span of antigenic area. The black bar above all tracks represents an 11 AA region of overlap in 100% (7/7) patients within the C-terminal domain. The amino acid sequence for the region of overlap is depicted above the black bar.

autoantibodies using whole cell lysates prepared from 293T cells overexpressing ZSCAN1. When Western blotting denatured lysates with CSF, we reproduce positive signal with 6/6 CSF (Fig 5).

### Testing Antigen Expression in Tumor and Brain

Typically, autoantibodies associated with PNS target antigens that are expressed in relevant tumor and healthy brain, otherwise known as onconeural antigens.<sup>46</sup> To test for tumor expression of ZSCAN1, 1 NT from ROHHAD-3 was sectioned and immunostained with a previously validated commercial antibody to ZSCAN1 (Fig 4). A rabbit secondary only control was used to test for nonspecific staining of rabbit IgG to infiltrating human IgG and Fc proteins in the tumor. ZSCAN1 expression was apparent in the ROHHAD-associated tumor (Fig 6). To test for hypothalamic expression of ZSCAN1, mass spectrometry analysis was performed using immunoprecipitation from human hypothalamic lysates using commercial antibodies to ZSCAN1. ZSCAN1 peptides were readily detectable, consistent with protein expression in this tissue (data available on Dryad repository).

### Discussion

In this work, we describe a proteome-wide screen for autoantibodies in patients with ROHHAD, a complex, diagnostically challenging syndrome with severe and often life-threatening symptoms.<sup>1, 2</sup> By comparing antibody profiles from ROHHAD patients to a large set of clinically relevant controls, we found autoantibodies to ZSCAN1 are a putative biomarker of ROHHAD and, thus, have potential utility in identifying ROHHAD earlier in the disease course.

All patients in this ROHHAD cohort (n = 9/9) exhibited the defining symptoms of the syndrome including rapid-onset obesity and hypothalamic dysfunction, with an onset between 2 to 5 years of age.<sup>1, 2</sup> NTs were present in 8/9 patients. Autoantibodies to ZSCAN1 were identified in 7 of 9 patients tested (sera n = 7/9, paired CSF n = 5/6) by PhIP-Seq, all of whom had NTs. Each of the 7 PhIP-Seq positive samples (ROHHAD-1 through -7) were validated by at least two orthogonal assays, including 293 T CBA and RLBA. Two assay validation limits the possibility of false-positive results and is increasingly accepted as a prerequisite for defining bona fide autoantigens.<sup>38, 47</sup>

Two ROHHAD patients (ROHHAD-8 and -9) were negative for ZSCAN1 autoantibodies, although CSF was not available for testing. Interestingly, ROHHAD-8 was in clinical remission when their sera was collected and at an older age (24 years) compared to other patients (age range = 2–10 years, median 3 years), who all exhibited active symptoms at sample collection. ROHHAD-9 did not have a tumor identified but exhibited the ROHHAD phenotype and active disease. Future experiments to determine the association of ZSCAN1 antibodies and ROHHAD syndrome in the absence of NT are warranted.

Previous clinical reports suggested ROHHAD could be a PNS by virtue of its co-occurrence with a tumor type already associated with a different PNS (OMS), clinical features of autoimmunity and the failure to identify consistent genetic associations.<sup>3, 7, 8, 16–19, 24, 26–31</sup> Our findings collectively support the notion of a PNS etiology. First, autoantibodies to the molecular antigen (ZSCAN1) were found in the majority (7/9) of



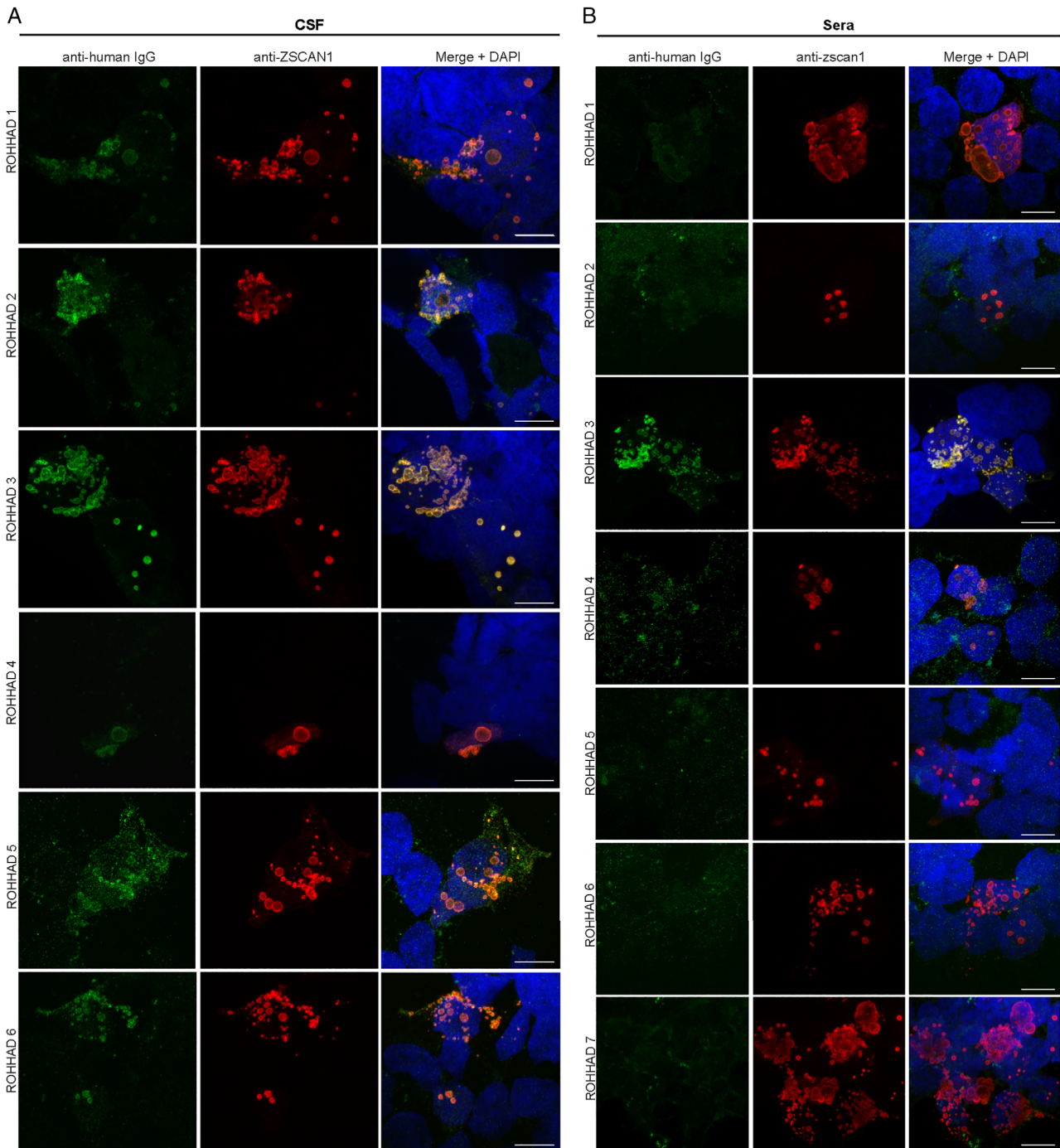


**FIGURE 4: Validation of ZSCAN1 autoantibodies in CSF and sera of ROHHAD patients using 293 T CBAs. (A) CSF:** Immunocytochemistry with 293T cells expressing full-length ZSCAN1 and immunostaining with CSF (1:10) from ROHHAD patients and commercial antibody to ZSCAN1 (rabbit, 1:1000 Invitrogen). Anti-human IgG-488 was used to visualize human IgG, and anti-rabbit IgG-567 was used to visualize anti-ZSCAN1 commercial antibody. Exposure times and post-image processing and thresholding was kept constant across conditions within the experiment. Co-localization was assessed qualitatively through observance of yellow in merged images. **(B) Sera:** Immunocytochemistry with 293T cells expressing full-length ZSCAN1 and immunostaining with sera (1:100) from ROHHAD patients and commercial antibody to ZSCAN1 (rabbit, 1:1000 Invitrogen). Anti-human IgG-488 was used to visualize human IgG, and anti-rabbit IgG-567 was used to visualize anti-ZSCAN1 commercial antibody. Exposure times and post-image processing and thresholding was kept constant across conditions within the experiment. Co-localization was assessed qualitatively through observance of yellow in merged images. Note colocalization in ROHHAD Sera-1 and -3.

INPUT (all lanes): 293T whole cell lysate expressing full length human ZSCAN1-FLAG

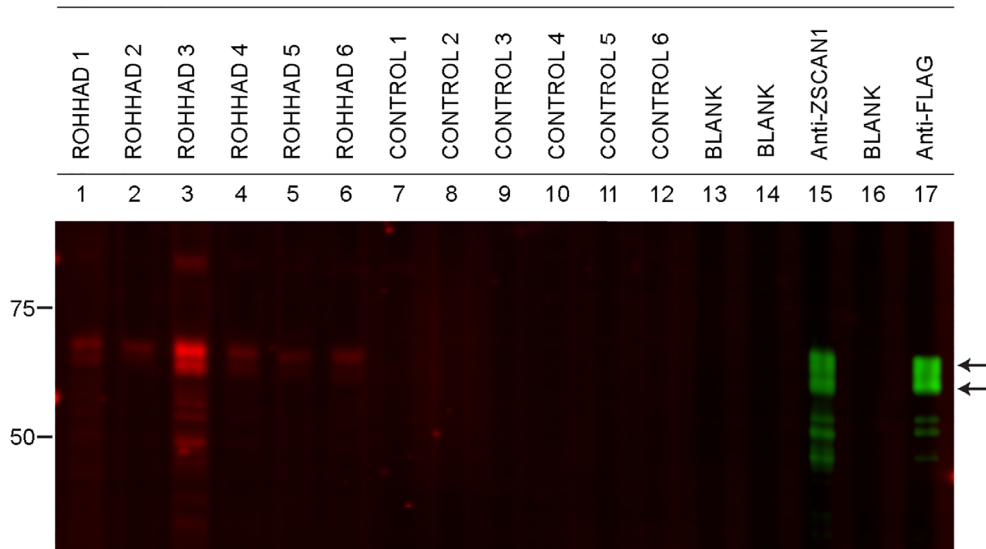


**FIGURE 5:** Detection of ZSCAN1 autoantibodies with slot-blot Western blotting using ROHHAD CSF. Whole cell-lysates from HEK293T cells expressing transfected with full-length human ZSCAN1 cDNA were separated on a 1-well 4–12% Tris-HCl protein gel, transferred to a PVDF membrane and immunoblotted in a slot-blot device (BioRad). Primary and secondary antibodies were added to lanes as indicated. Primary antibodies were loaded in lanes 1–12. Lanes 13 and 15 served as secondary-only controls. Primary antibodies are as follows: lanes 1 through 7: ROHHAD 1 through 7 CSF (1:200); lanes 8 through 12: controls 1–5 CSF (1:200); lane 13: blank; lane 14: commercial antibody to ZSCAN1 (Sigma, rabbit, 1:2000); lane 15: blank, lane 16: commercial antibody to Flag (CST, rabbit, 1:2000). Secondary antibodies to visualize human IgG loaded in lanes 1–12: goat anti-human IgG (LICOR680). Secondary antibodies to visualize commercial antibodies to ZSCAN1 and FLAG lanes 14 and 16: goat anti-rabbit IgG (LICOR800).

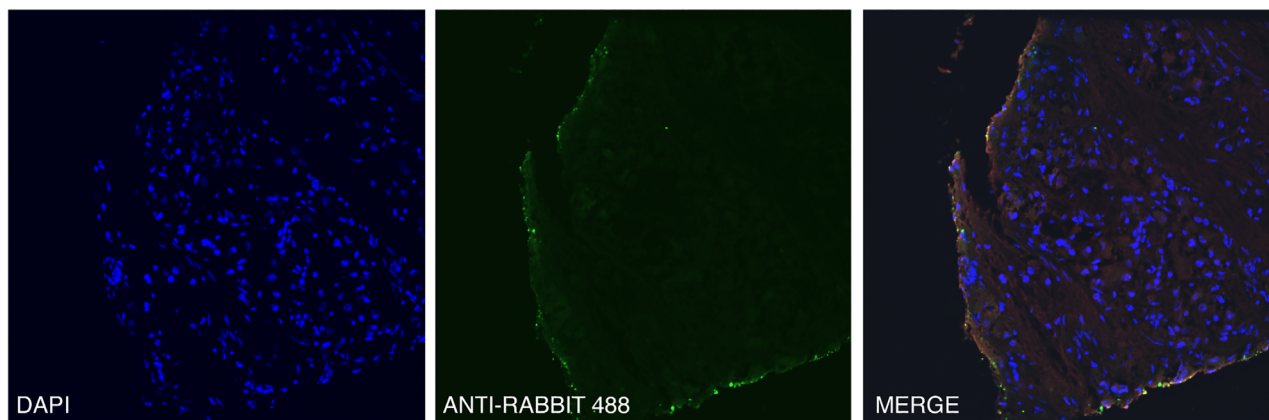
ROHHAD cases, and in all from cases with a NT identified. The robust association of ZSCAN1 autoantibodies (>70% of patients) with NT associated ROHHAD fulfills the new diagnostic criteria for PNS etiology.<sup>48</sup> Second, ZSCAN1 expression in human hypothalamus is consistent with the target tissues affected in ROHHAD patients. Third, ZSCAN1 was found to be expressed in NT tissue from a patient with ROHHAD. Fourth, the presumed intracellular localization of ZSCAN1 ([www.uniprot.org](http://www.uniprot.org), [www.proteinatlas.org](http://www.proteinatlas.org)), together with expression in ROHHAD NTs as well as healthy nervous system tissue, is reminiscent of other classical PNS onconeural antigens. Antibodies to intracellular onconeural antigens are a biomarker for a major subtype of PNS, such as cerebellar degeneration-related protein 2-like in anti-Yo PNS and neuronal ELAV-like proteins 2,3,4 in anti-Hu PNS<sup>33</sup>. In these cases, autoantibodies themselves are not thought to be directly pathogenic, and the diseases are often less consistently responsive to tumor resection and immunosuppressive therapy compared to PNS with antibodies to extracellular antigens. Consistent with the hypothesis of PNS, ROHHAD patients have variable responses (duration and magnitude) to immunosuppressive therapy or tumor resection and may respond better to earlier, more aggressive regimens.<sup>3, 7, 30, 31</sup>

The ZSCAN1 protein is a putative zinc finger transcription factor (znTF) that contains a single SCAN domain and three Cysteine2-Histidine2 (C2H2) zinc finger domains ([uniprot.org](http://uniprot.org)). Despite nearly equal representation of SCAN domain (84 AA) and C2H2 domains (100 AA), antigenicity in ZSCAN1 is biased to the C2H2 domains, a functional region for DNA and RNA binding<sup>49</sup> (Fig 3). Furthermore, although ~700 human proteins containing C2H2 domains with the motif C-X2-4-C-X12-H-X2-6-H (where X is any AA) are present in our PhIP-Seq library, no other ZnTFs were significantly enriched in more than one patient (Z-score >1), highlighting the specificity of the motif identified by PhIP-Seq. Importantly, the ZSCAN1 gene lacks a genetic ortholog in rodents, including mice and rats, with evolutionary divergence towards primate-specificity in the C2H2 region.<sup>49–51</sup> These observations suggest the putative epitope within ZSCAN1 has a high likelihood of being exclusive to primates. To our knowledge, a primate-specific epitope in autoimmune disease has not yet been described.

A common autoantibody among ROHHAD patients suggests a route to a molecular diagnostic. Here we demonstrate the value of the human-specific PhIP-Seq approach for ROHHAD biomarker discovery. ZSCAN1 has no genetic ortholog in rodents, so the classical rodent based approach for PNS autoantibody detection failed.

## ROHHAD-003 Neuroblastic Tumor

### Secondary only control ( No primary Ab + Anti-Rabbit-488 secondary + DAPI)



### Anti- ZSCAN1 primary Ab (Rabbit) + Anti-Rabbit-488 secondary + DAPI

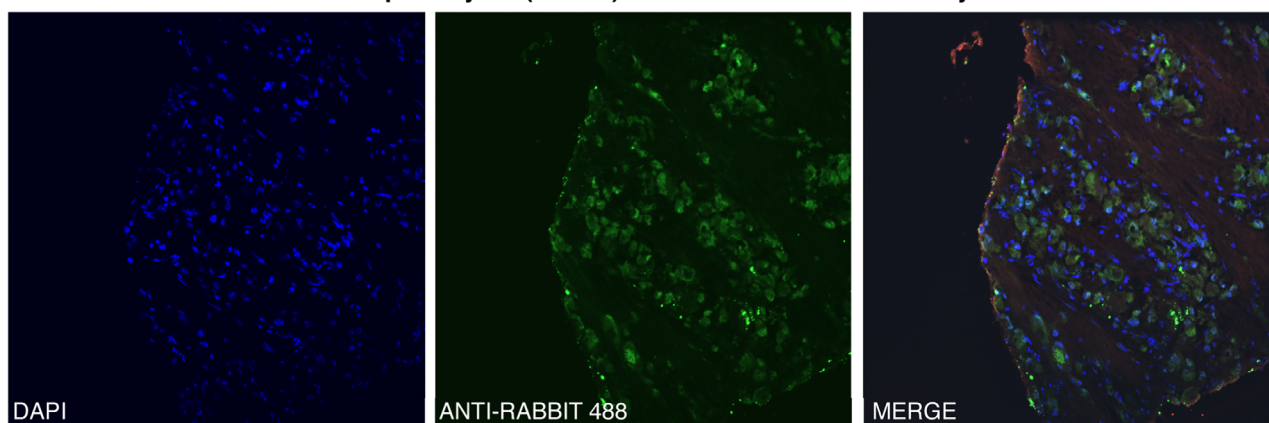


**FIGURE 6:** Immunohistochemical detection of ZSCAN1 in NT associated with ROHHAD patient-3. Fixed neuroblastoma tissue was immunostained with either (top) anti-rabbit-488 secondary alone or (bottom) primary antibody to ZSCAN1 (rabbit) and anti-rabbit-488 secondary. Green: anti-rabbit-488 secondary; blue: DAPI (4'-6'-diamidino-2-phenylindole) to identify nuclei.

Our results suggest CBAs or RLBA on CSF may be sufficient to detect ZSCAN1 autoantibodies in a clinical lab setting and could be offered as a stand-alone test or added to existing paraneoplastic antibody panels. In the case of ROHHAD, these results also suggest that CSF may be the most sensitive sample type for testing, since ZSCAN1 was not always detectable in sera, particularly on CBA, as is true for many PNSs.

To summarize, we provide a robust finding of autoantibodies to ZSCAN1 as a marker for tumor-associated pediatric ROHHAD. ZSCAN1 expression in tumor and human hypothalamus provides further evidence to support the clinical suspicion that ROHHAD is a novel type of PNS. This is the first identified intracellular antigen in a PNS unique to children. Further experiments are required to test the utility of ZSCAN1 autoantibodies for diagnosis in ROHHAD patients with and without tumors and NTs without paraneoplastic syndromes, define the clinical spectrum of PNS ROHHAD, and to understand how

immune targeting of ZSCAN1 contributes to the dramatic clinical complications seen in patients with ROHHAD syndrome.

### Acknowledgments

This research was supported by ROHHAD Fight, Inc, the Shore Foundation, the OMS Life Foundation, the Repository Core for Neurological Disorders, Department of Neurology, Boston Children's Hospital, and the IDDRRC (NIH P30HD018655) and NIH R01MH122471. We also acknowledge the New York Blood Center for contribution of healthy control plasma. Instituto Carlos III (ISCIII, PI20/00197 [JD]), and "La Caixa" Foundation (JD). C.M.A. is supported by NIDDK (K23DK120899). Acknowledge the UCSF Nikon Core Facility for microscope imaging equipment and guidance. J.D.L. is funded by a grant from Chan Zuckerberg Biohub. J.D.L., M.R.W., S.J.P., and C.M.B. are funded by the National

Institute of Mental Health (NIMH) of the NIH (award 1R01MH122471-01). S.J.P. and B.T. are also funded by the Brain Research Foundation (Scientific Innovations Award). C.M.B. is also funded by The Emiko Terasaki Foundation (Project 7027742 / Fund B73335) and by the National Institute of Neurological Disorders and Stroke (NINDS) of the National Institutes of Health (award 1K99NS117800-01). S.E.V. is funded by the National Institute of Diabetes and Digestive and Kidney Diseases of the NIH (award 1F30DK123915-01).

## Author Contributions

C.M.B., L.B. and B.T. contributed equally to this work including drafting of the manuscript. L.B., M.P.G., J.D.R., M.R.W. and S.J.P. contributed to the conception and design of the study; C.M.B., S.A.M., H.R. A.F.K., B.T., S.E.V., P.L.M., L.Z., F.M., J.E.E., W.W.S., J.D., H.A.S., K.C.Z., L.M.K., U.K., C.M.A., S.T., L.M.K., M.R.W. contributed to the acquisition and analysis of data; L.B., L.M.K., C.M., B.T. contributed to drafting the text and/or preparing the figures.

## Conflicts of Interest

Nothing to report.

## References

- Katz ES, McGrath S, Marcus CL. Late-onset central hypoventilation with hypothalamic dysfunction: a distinct clinical syndrome. *Pediatr Pulmonol* 2000;29:62–68. [https://doi.org/10.1002/\(sici\)1099-0496\(200001\)29:1<62::aid-ppul10>3.0.co;2-m](https://doi.org/10.1002/(sici)1099-0496(200001)29:1<62::aid-ppul10>3.0.co;2-m).
- Ize-Ludlow D, Gray JA, Sperling MA, et al. Rapid-onset obesity with hypothalamic dysfunction, hypoventilation, and autonomic dysregulation presenting in childhood. *Pediatrics* 2007;120:e179–e188. <https://doi.org/10.1542/peds.2006-3324>.
- Ibanez-Mico S, Marcos Oltra AM, de Murcia LS, et al. Rapid-onset obesity with hypothalamic dysregulation, hypoventilation, and autonomic dysregulation (ROHHAD syndrome): a case report and literature review. *Neurologia* 2017;32:616–622. <https://doi.org/10.1016/j.nrl.2016.04.008>.
- Patwari PP, Wolfe LF. Rapid-onset obesity with hypothalamic dysfunction, hypoventilation, and autonomic dysregulation: review and update. *Curr Opin Pediatr* 2014;26:487–492. <https://doi.org/10.1097/MOP.000000000000118>.
- Lee JM, Shin J, Kim S, et al. Rapid-onset obesity with hypoventilation, hypothalamic, autonomic dysregulation, and neuroendocrine tumors (ROHHADNET) syndrome: a systematic review. *Biomed Res Int* 2018;2018:1250721–1250717. <https://doi.org/10.1155/2018/1250721>.
- Chew HB, Ngu LH, Keng WT. Rapid-onset obesity with hypothalamic dysfunction, hypoventilation and autonomic dysregulation (ROHHAD): a case with additional features and review of the literature. *BMJ Case Rep* 2011;2011:bcr0220102706. <https://doi.org/10.1136/bcr.02.2010.2706>.
- Jacobson LA, Rane S, McReynolds LJ, et al. Improved behavior and neuropsychological function in children with ROHHAD after high-dose cyclophosphamide. *Pediatrics* 2016;138:e1–e5. <https://doi.org/10.1542/peds.2015-1080>.
- Sethi K, Lee YH, Daugherty LE, et al. ROHHADNET syndrome presenting as major behavioral changes in a 5-year-old obese girl. *Pediatrics* 2014;134:e586–e589. <https://doi.org/10.1542/peds.2013-2582>.
- Jalal Eldin AW, Tombayoglu D, Butz L, et al. Natural history of ROHHAD syndrome: development of severe insulin resistance and fatty liver disease over time. *Clin Diabet Endocrinol* 2019;5:9. <https://doi.org/10.1186/s40842-019-0082-y>.
- Stowe RC, Afolabi-Brown O. Pulmonary hypertension and chronic hypoventilation in ROHHAD syndrome treated with average-volume assured pressure support. *Pediatr Investig* 2019;3:253–256. <https://doi.org/10.1002/ped4.12168>.
- Selvadurai S, Benzon D, Voutsas G, et al. Sleep-disordered breathing, respiratory patterns during wakefulness and functional capacity in pediatric patients with rapid-onset obesity with hypothalamic dysfunction, hypoventilation and autonomic dysregulation syndrome. *Pediatr Pulmonol* 2021;56:479–485. <https://doi.org/10.1002/ppul.25199>.
- Kocaay P, Siklar Z, Camtosun E, et al. ROHHAD syndrome: reasons for diagnostic difficulties in obesity. *J Clin Res Pediatr Endocrinol* 2014;6:254–257. <https://doi.org/10.4274/Jcrpe.1432>.
- Barclay SF, Rand CM, Nguyen L, et al. ROHHAD and Prader-Willi syndrome (PWS): clinical and genetic comparison. *Orphanet J Rare Dis* 2018;13:124. <https://doi.org/10.1186/s13023-018-0860-0>.
- Barclay SF, Rand CM, Gray PA, et al. Absence of mutations in HCRT, HCRT1 and HCRT2 in patients with ROHHAD. *Respir Physiol Neurobiol* 2016;221:59–63. <https://doi.org/10.1016/j.resp.2015.11.002>.
- Cielo C, Marcus CL. Central hypoventilation syndromes. *Sleep Med Clin* 2014;9:105–118. <https://doi.org/10.1016/j.jsmc.2013.10.005>.
- Barclay SF, Rand CM, Borch LA, et al. Rapid-onset obesity with hypothalamic dysfunction, hypoventilation, and autonomic dysregulation (ROHHAD): exome sequencing of trios, monozygotic twins and tumours. *Orphanet J Rare Dis* 2015;10:103. <https://doi.org/10.1186/s13023-015-0314-x>.
- Patwari PP, Rand CM, Berry-Kravis EM, et al. Monozygotic twins discordant for ROHHAD phenotype. *Pediatrics* 2011;128:e711–e715. <https://doi.org/10.1542/peds.2011-0155>.
- Rand CM, Patwari PP, Rodikova EA, et al. Rapid-onset obesity with hypothalamic dysfunction, hypoventilation, and autonomic dysregulation: analysis of hypothalamic and autonomic candidate genes. *Pediatr Res* 2011;70:375–378. <https://doi.org/10.1203/PDR.0b013e318229474d>.
- Thaker VV, Esteves KM, Towne MC, et al. Whole exome sequencing identifies RAI1 mutation in a morbidly obese child diagnosed with ROHHAD syndrome. *J Clin Endocrinol Metab* 2015;100:1723–1730. <https://doi.org/10.1210/jc.2014-4215>.
- Harvengt J, Gemay C, Mastouri M, et al. ROHHAD(NET) Syndrome: systematic review of the clinical timeline and recommendations for diagnosis and prognosis. *J Clin Endocrinol Metab* 2020;105:2119–2131. <https://doi.org/10.1210/clinem/dgaa247>.
- Zaidi S, Gandhi J, Vatsia S, et al. Congenital central hypoventilation syndrome: an overview of etiopathogenesis, associated pathologies, clinical presentation, and management. *Auton Neurosci* 2018;210:1–9. <https://doi.org/10.1016/j.autneu.2017.11.003>.
- Meena JP, Seth R, Chakrabarty B, et al. Neuroblastoma presenting as opsoclonus-myoclonus: a series of six cases and review of literature. *J Pediatr Neurosci* 2016;11:373–377. <https://doi.org/10.4103/1817-1745.199462>.
- Rudnick E, Khakoo Y, Antunes NL, et al. Opsoclonus-myoclonus-ataxia syndrome in neuroblastoma: clinical outcome and antineuronal antibodies—a report from the Children's cancer group study. *Med Pediatr Oncol* 2001;36:612–622. <https://doi.org/10.1002/mpo.1138>.
- Gharia J, Ganesh A, Curtis C, et al. Neuroimaging and pathology findings associated with rapid onset obesity, hypothalamic dysfunction, hypoventilation, and autonomic dysregulation (ROHHAD)

- syndrome. *J Pediatr Hematol Oncol* 2021;43:e571–e576. <https://doi.org/10.1097/MPH.0000000000001927>.
25. Nunn K, Ouvrier R, Sprague T, et al. Idiopathic hypothalamic dysfunction: a paraneoplastic syndrome? *J Child Neurol* 1997;12:276–281. <https://doi.org/10.1177/088307389701200412>.
  26. Cemeroglu AP, Eng DS, Most LA, et al. Rapid-onset obesity with hypothalamic dysfunction, hypoventilation, and autonomic dysregulation syndrome and celiac disease in a 13-year-old girl: further evidence for autoimmunity? *J Pediatr Endocrinol Metab* 2016;29:97–101. <https://doi.org/10.1515/jpem-2015-0129>.
  27. Sirvent N, Berard E, Chastagner P, et al. Hypothalamic dysfunction associated with neuroblastoma: evidence for a new paraneoplastic syndrome? *Med Pediatr Oncol* 2003;40:326–328. <https://doi.org/10.1002/mpo.10157>.
  28. Sartori S, Priante E, Pettenazzo A, et al. Intrathecal synthesis of oligoclonal bands in rapid-onset obesity with hypothalamic dysfunction, hypoventilation, and autonomic dysregulation syndrome: new evidence supporting immunological pathogenesis. *J Child Neurol* 2014;29:421–425. <https://doi.org/10.1177/0883073812469050>.
  29. Armangue T, Petit-Pedrol M, Dalmau J. Autoimmune encephalitis in children. *J Child Neurol* 2012;27:1460–1469. <https://doi.org/10.1177/0883073812448838>.
  30. Paz-Priel I, Cooke DW, Chen AR. Cyclophosphamide for rapid-onset obesity, hypothalamic dysfunction, hypoventilation, and autonomic dysregulation syndrome. *J Pediatr* 2011;158:337–339. <https://doi.org/10.1016/j.jpeds.2010.07.006>.
  31. Huppke P, Heise A, Rostasy K, et al. Immunoglobulin therapy in idiopathic hypothalamic dysfunction. *Pediatr Neurol* 2009;41:232–234. <https://doi.org/10.1016/j.pediatrneurol.2009.03.017>.
  32. Voltz R. Paraneoplastic neurological syndromes: an update on diagnosis, pathogenesis, and therapy. *Lancet Neurol* 2002;1:294–305. [https://doi.org/10.1016/s1474-4422\(02\)00135-7](https://doi.org/10.1016/s1474-4422(02)00135-7).
  33. Dalmau J, Graus F. Antibody-mediated encephalitis. *N Engl J Med* 2018;378:840–851. <https://doi.org/10.1056/NEJMr1708712>.
  34. Giacomozzi C, Guaraldi F, Cambiaso P, et al. Anti-hypothalamus and anti-pituitary auto-antibodies in ROHHAD syndrome: additional evidence supporting an autoimmune etiopathogenesis. *Horm Res Paediatr* 2019;92:124–132. <https://doi.org/10.1159/000499163>.
  35. Mandel-Brehm C, Dubey D, Kryzer TJ, et al. Kelch-like protein 11 antibodies in seminoma-associated paraneoplastic encephalitis. *N Engl J Med* 2019;381:47–54. <https://doi.org/10.1056/NEJMoa1816721>.
  36. Zhao Y, Tang H, Ye Y. RAPSearch2: a fast and memory-efficient protein similarity search tool for next-generation sequencing data. *Bioinformatics* 2012;28:125–126. <https://doi.org/10.1093/bioinformatics/btr595>.
  37. Rathore GS, Thompson-Stone RI, Benson L. Chapter 20: rapid-onset obesity with hypothalamic dysfunction, hypoventilation, and autonomic dysregulation (ROHHAD). In: Waubant ELT, ed. *Pediatric demyelinating diseases of the central nervous system and their mimics: a case-based clinical guide*. 1st ed. Switzerland: Springer International Publishing; 2017.
  38. Dalmau J, Posner JB. Neurologic paraneoplastic antibodies (anti-Yo; anti-Hu; anti-Ri): the case for a nomenclature based on antibody and antigen specificity. *Neurology* 1994;44:2241–2246. <https://doi.org/10.1212/wnl.44.12.2241>.
  39. Lennon VA. The case for a descriptive generic nomenclature: clarification of immunostaining criteria for PCA-1, ANNA-1, and ANNA-2 autoantibodies. *Neurology* 1994;44:2412–2415. <https://doi.org/10.1212/wnl.44.12.2412>.
  40. Darnell RB, Posner JB. Paraneoplastic syndromes involving the nervous system. *N Engl J Med* 2003;349:1543–1554. <https://doi.org/10.1056/NEJMr023009>.
  41. Ances BM, Vitaliani R, Taylor RA, et al. Treatment-responsive limbic encephalitis identified by neuropil antibodies: MRI and PET correlates. *Brain* 2005;128:1764–1777. <https://doi.org/10.1093/brain/awh526>.
  42. Lai M, Hughes EG, Peng X, et al. AMPA receptor antibodies in limbic encephalitis alter synaptic receptor location. *Ann Neurol* 2009;65:424–434. <https://doi.org/10.1002/ana.21589>.
  43. O'Donovan B, Mandel-Brehm C, Vazquez SE, et al. High-resolution epitope mapping of anti-Hu and anti-Yo autoimmunity by programmable phage display. *Brain Commun* 2020;2:fcaa059. <https://doi.org/10.1093/braincomms/fcaa059>.
  44. Vazquez SE, Ferre EM, Scheel DW, et al. Identification of novel, clinically correlated autoantigens in the monogenic autoimmune syndrome APS1 by proteome-wide PhIP-Seq. *Elife* 2020;9:1–25. <https://doi.org/10.7554/eLife.55053>.
  45. Ruiz-Garcia R, Martinez-Hernandez E, Saiz A, et al. The diagnostic value of Onconeural antibodies depends on how they are tested. *Front Immunol* 2020;11:1482. <https://doi.org/10.3389/fimmu.2020.01482>.
  46. Dalmau JO, Posner JB. Paraneoplastic syndromes affecting the nervous system. *Semin Oncol* 1997;24:318–328.
  47. Ruiz-Garcia R, Martinez-Hernandez E, Garcia-Ormaechea M, et al. Caveats and pitfalls of SOX1 autoantibody testing with a commercial line blot assay in paraneoplastic neurological investigations. *Front Immunol* 2019;10:769. <https://doi.org/10.3389/fimmu.2019.00769>.
  48. Graus F, Vogrig A, Muniz-Castrillo S, et al. Updated diagnostic criteria for paraneoplastic neurologic syndromes. *Neurol Neuroimmunol Neuroinflamm* 2021;8:e1014. <https://doi.org/10.1212/NXI.0000000000001014>.
  49. Iuchi S. Three classes of C2H2 zinc finger proteins. *Cell Mol Life Sci* 2001;58:625–635. <https://doi.org/10.1007/PL00000885>.
  50. Dehal P, Predki P, Olsen AS, et al. Human chromosome 19 and related regions in mouse: conservative and lineage-specific evolution. *Science* 2001;293:104–111. <https://doi.org/10.1126/science.1060310>.
  51. Sander TL, Stringer KF, Maki JL, et al. The SCAN domain defines a large family of zinc finger transcription factors. *Gene* 2003;310:29–38. [https://doi.org/10.1016/s0378-1119\(03\)00509-2](https://doi.org/10.1016/s0378-1119(03)00509-2).